MOCVD Regrown Ohmic Contacts to AlGaN/GaN Heterostructures

Savannah Benbrook (sbenbroo@stanford.edu)
Yanni Dahmani (ydahmani@stanford.edu)
Mentor: Dr. Xiaqing Xu
Spring 2018

Abstract: AlGaN/GaN transfer length method (TLM) and Hall devices were fabricated with n+ doped GaN recessed Ohmic contact regions by metal-organic chemical vapor deposition (MOCVD) regrowth technology. The impact of MOCVD regrowth temperature and precursor flow rates on the quality and growth rate of n+ GaN were qualitatively evaluated through scanning electron microscopy (SEM). Ti/Al/Pt/Au metallized regrown n+ GaN Ohmic contacts exhibited a minimum specific contact resistivity of 1.3×10^{-3} Ωcm^2 and sheet resistance of 150 Ω/sq. It is hypothesized that carbon traces remaining on the AlGaN/GaN samples prior to re-entering the MOCVD chamber for regrowth is the cause of abnormal porous regions and defect density in the n+GaN film and the subsequently high specific contact resistivities.

I. Introduction & Motivation

Gallium Nitride (GaN)-based heterostructures are frequently employed in high-frequency, high-power, and optoelectronic devices due to their wide bandgap, high breakdown voltage, high electron saturation velocity, and high thermal conductivity [1]. Furthermore, GaN heterostructured devices have demonstrated thermal stability up to 1000C in vacuum, making GaN-based devices of great interest to the high-temperature device community and enabling their use in extreme environment applications where traditional semiconductor materials like Silicon cannot survive, such as Venus exploration [2]. However, current GaN-based device reliability is dominated not by the robust heterostructured material itself, but by the accompanying contact metallization schemes. High contact resistance and failure caused by interdiffusion, outdiffusion and contact sinking in traditional metallization schemes on GaN-heterostructures have driven the need for new approaches to metallization.

Literature has demonstrated ohmic contact formation via MOCVD "regrowth" of an n+ GaN layer to side contact to the 2DEG on AlGaN/GaN substrates is a promising approach to reducing the contact resistance of GaN heterostructures [3b][4][5]. Low Ohmic contact resistances on the order of tenths of Ohms/mm have been reported [6][7]. The goal of this project was to develop an ohmic contact regrowth technique for GaN heterostructures suitable for SNF equipment and cleanliness requirements. This technique had yet to be performed in the SNF due to contamination concerns associated with the MOCVD regrowth step. An initial strategy had been outlined with Xiaoqing with guidance from Usha for methodically evaluating an MOCVD

regrowth technique with an emphasis on maintaining the cleanliness-level of the Oxford III-V and MOCVD systems. The project afforded the opportunity to develop new capabilities within the SNF as well as a deep-dive into device surface contamination and characterization techniques. MOCVD regrowth capability will not only enable the formation of low resistance contacts on GaN-based devices, but can also be leveraged for other applications in the future.
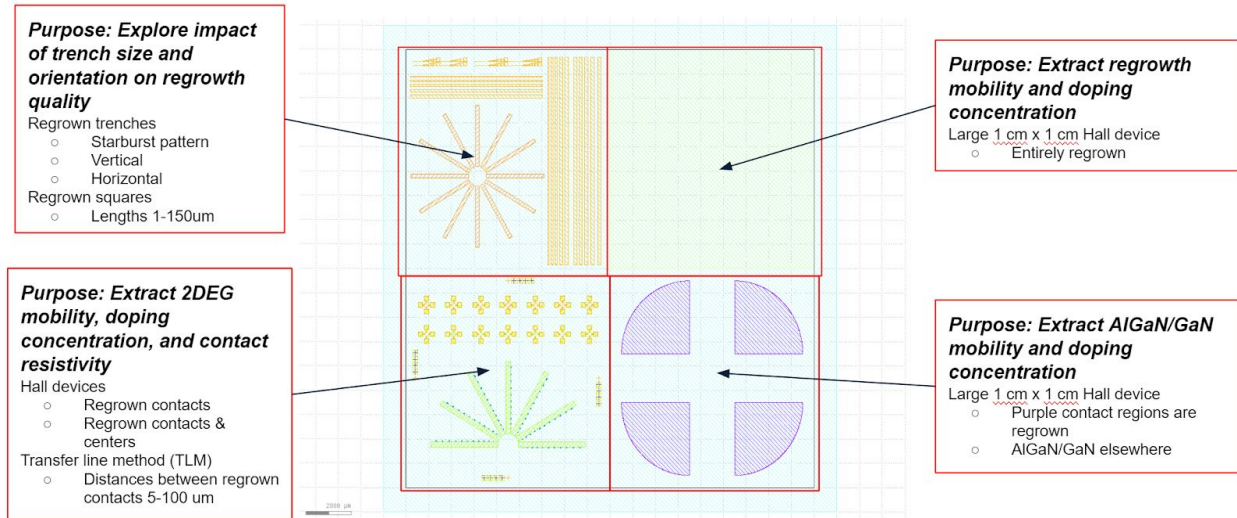
II. Process
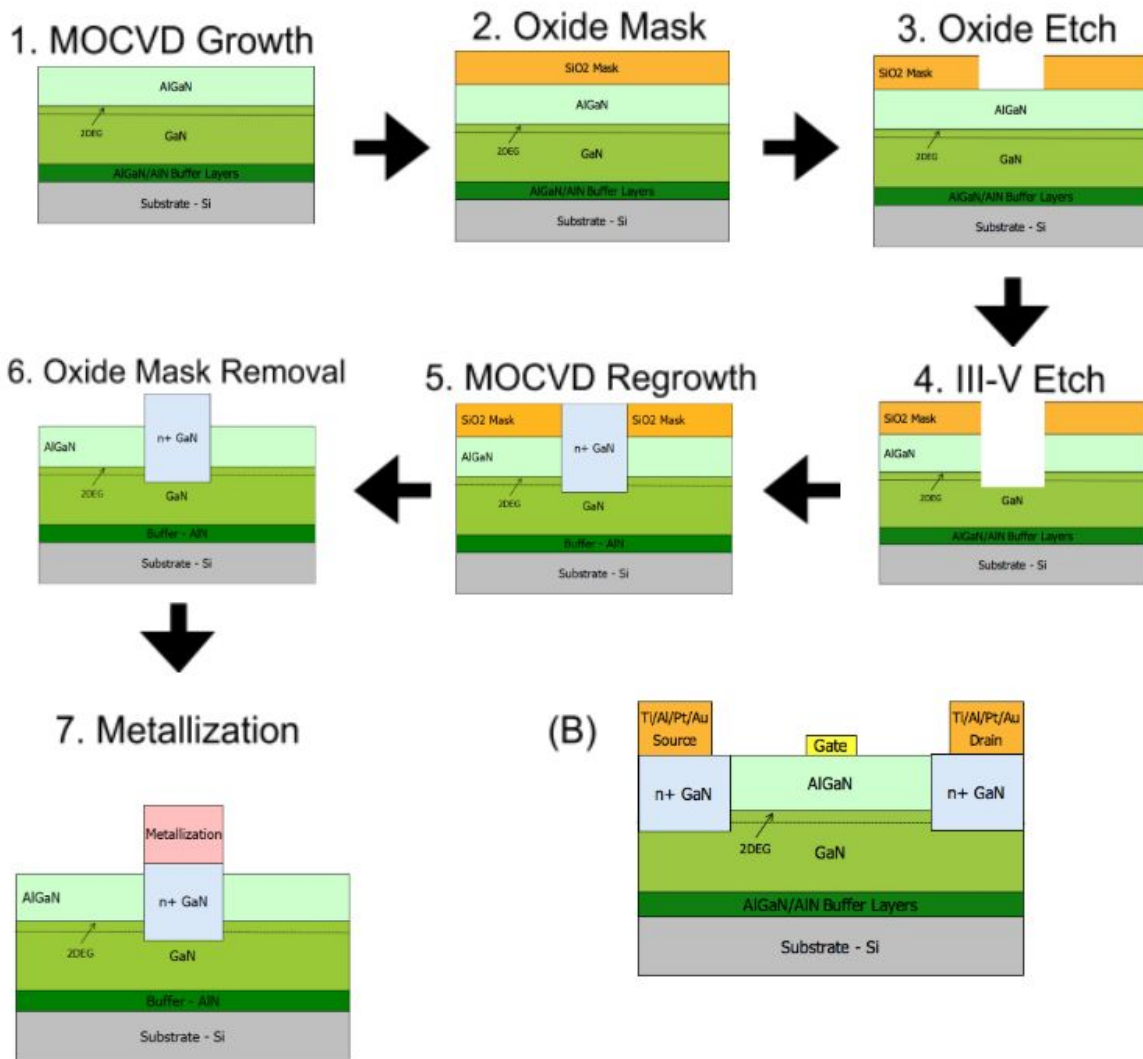
Figure 1: (A) Process flow for the MOCVD regrown ohmic contacts. (B) Cross section of an AlGaN/GaN HEMT with regrown n+ GaN to ohmic contact metallization.

The simplified fabrication flow can be seen in Fig. 1. AlGaN/GaN was grown on a 4" clean p-type Si(111) wafer through MOCVD. After growth a SiO2 mask approximately 150nm thick was deposited through plasma-enhanced chemical vapor deposition (PECVD) in the CCP. The CCP tool falls in the flexible category and was converted to clean through a standard procedure. It is key that the sample remain clean prior to reentering the MOCVD chamber for regrowth due to the high cleanliness required for the high temperature chemical vapor deposition for two reasons. First, the quality of MOCVD grown thin film n+ GaN is suspected to be severely degraded by the presence of particles on the sample surface. Secondly, as mentioned above contamination of the MOCVD chamber is a key concern because the growths performed by other users of the tool could also be adversely affected. However, samples that have been placed in the MOCVD chamber are not considered to be in the clean category by the SNF, and therefore are not eligible for processing in clean pieces of equipment. Thus, the etch of the oxide hard mask was performed in the gold contaminated Ox-RIE reactive ion etcher. Prior to using the Ox-RIE, the chamber was manually cleaned by SNF staff member Elmer Enriquez to attempt to minimize the contamination seen by our sample. The clean consisted of an Isopropanol wipedown followed by an O2 plasma clean and seasoning with our recipe of choice. The Oxford III-V, another gold-contaminated tool but the only reasonable option for notoriously hard to etch GaN, was cleaned in the same fashion as the Ox-RIE. The AlGaN/GaN was etched to various depths with the goal of n+ GaN sidecontacting to the 2DEG present in the AlGaN/GaN. After extensive wet processing to try to remove gold and organic contaminants that may be present on the sample both between the Ox-RIE and Ox III-V and after the Ox III-V, samples were placed back in the MOCVD one at a time for growth of n+ GaN in the recessed trenches patterned in the oxide hard mask and exposed GaN. The presence of the oxide mask was to protect areas of the AlGaN/GaN during MOCVD where n+ GaN was not wanted to grow. A design of experiments was performed to optimize the n+ GaN MOCVD recipe and is described in the next section. After regrowth, the sample no longer had to remain as clean as possible and contamination was no longer a concern. The oxide mask was removed by a 50:1 HF etch in SNF gold-contaminated beakers. Following the removal of the mask, regrowths #3 and #4 were subjected to further processing in preparation for electrical characterization. This consisted of a mesa etch to isolate the TLM structures, meaning the AlGaN/GaN was etched down far enough so that the 2DEG no longer existed on the samples except in the regions between the TLM contacts where the current should be confined to flowing. After the mesa etch, the TLM structures were patterned once more and underwent electron beam evaporation of 20nm/100nm/40nm/80nm Ti/Al/Pt/Au in the AJA along with the two 1 cm x 1cm Hall devices that were patterned using a shadow mask. Following liftoff and rapid thermal anneal for 35 seconds at 850C, the Hall devices and the TLM structures were electrically characterized.

The full fabrication process can be found in the following spreadsheet:

III. Sample Design

Figure 2: The main mask design used throughout fabrication. The design was split into four sections that were diced after regrowth and underwent subsequent unique processes. The top left consisted of numerous trenches of various lengths, widths, and orientation and was used to determine trench widths, length, and orientation effects on regrowth quality. The bottom left consisted of numerous small Hall devices that could be wire-bonded to in the future, and TLM devices that the specific contact resistivity was later extracted from. The two right sections of the mask were dedicated to large hall devices to measure regrowth mobility and doping concentration (top right) and AlGaN/GaN mobility and doping concentration (bottom right).

All processes done on the AlGaN/GaN chips were governed by the mask design employed, shown in Figure 2. The 2 cm x 2 cm mask design was split into four 1 cm x 1 cm designs that were diced after regrowth, each with their own patterns and experimental purpose. The top left of the mask was dedicated to characterizing regrown n+ GaN quality and the effects of trench width, length, and orientation.. Numerous square trenches were etched with widths and heights ranging from 1 um to 150 um to see regrowth conditions in square trenches at various dimensions. Furthermore several horizontal and vertical trenches with varying widths—25 um to 150 um—as well as various spacings—75 to 150 um—were etched to see trench width and spacing effects on regrowth. A spiral trench pattern with angles of 30 degrees between two trenches was also etched to test trench orientation's effect on regrowth.

The bottom left pattern consisted solely of electrical characterization devices. Several small hall devices were patterned to measure the 2DEG mobility, doping concentration, and

contact resistivity - yet, these devices were intended as a backup method to extract this information because they require wire bonding services. Furthermore spiral Transfer Length Method (TLM) structures were patterned with the same angle spacing as the spiral trench mentioned above. The contact widths and heights of the TLM structure were 200 um by 220 um. Each contact within a single TLM structure was spaced by a different length in the range of 5-100 um.

The right two patterns were designed to test the mobility and doping concentration of the n+ GaN and the AlGaN/GaN heterostructure. The top right portion of the entire pattern was not protected the SiO2 during regrowth and the n+ GaN grew everywhere. Therefore, Hall measurements would give information on the mobility and doping of the n+ GaN. The bottom right portion of the sample had semicircles exposed during regrowth of n+GaN but the AlGaN/GaN was otherwise protected, thereby this device simulated actual n+GaN contacts to AlGaN/GaN. The 2DEG mobility and the doping concentration of the AlGaN/GaN could be extracted from this Hall device.

IV. Regrowth Design of Experiments (DOE)

Our design of experiments revolved around the parameters of the MOCVD during regrowth. Overall we did four regrowths within which we varied certain parameters such as the growth temperature and precursor flow rate. These values can be seen in Table 1. For all four growth processes the bake and anneal steps were the same. Each regrowth had a bake step which consisted of a 840 C bake at H_2 and three SLM of NH_3 for five minutes. Following this an anneal step took place which consisted of a 930 C anneal in N_2 and 5 SLM of NH_3 for 30 minutes in order to try to regain better surface morphology of the dry-etched trench sidewalls. The growth temperatures are what differed for each regrowth sample. Regrowth for sample one was grown on a two cm by two cm die patterned by the mask detailed in the above section. The growth was done at a temperature of 885 C in H_2 and NH_3. Regrowth for sample two was also done on a two cm by two cm die patterned with the mask and was grown at a temperature of 1090 C in H_2 and NH_3. Regrowth for sample three was done on a one cm by one cm piece that was cleaved off from that larger die and was patterned with the TLM structures in the mask design. The growth temperature was changed to 1050 C and the precursor flow rate was doubled to counteract the decomposition rate of the precursors at the high growth temperature. Finally regrowth sample four had the same recipe as regrowth sample three but was done on the full sample die with the full mask.

Regrowth #	Sample Size	Bake	Anneal	Growth Temp - H_2 and NH_3 ambient

| 1	2 cm x 2 cm	840°C H_2 ambient; 3 SLM NH_3 ambient for 5min	930°C N_2 ambient; 5 SLM NH_3 for 30min	885°C
2	2 cm x 2 cm			1090°C
3	Cleaved piece			1050°C; *TMGa, NH_3, SiH_4 flow rates doubled to counteract decomposition rate
4	2 cm x 2 cm			

Table 1: Regrowth MOCVD DOE recipes.

V. Characterization of Regrowth
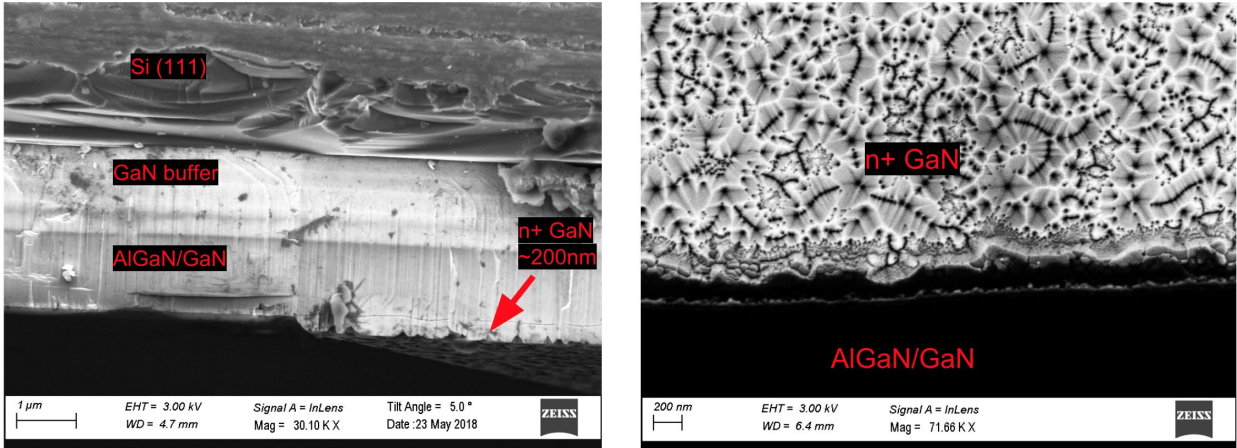
Figure 3: SEMs of the cross-section and top view of Regrowth 1. The cross-section shows the various layers in the AlGaN/GaN stack - the images were taken upside down. The measured growth was approximately 200 nm as shown in the SEM. The top view SEM shows the nonuniform, porous growth pattern of the regrown nGaN. The growth quality was thus determined to be poor.

Characterization of the regrowth was done through SEM images. Top view SEMs allowed us to see the uniformity of the regrowth at the top surface while cross-section SEMs allowed us to see the regrowth quality throughout the regrowth layer, as well as seeing sidewall growth and measuring regrowth heights. A top view and cross-section SEM of Regrowth 1 can be seen in Figure 3. Regrowth 1 exhibited poor regrowth quality as the top view showed a highly

non-uniform and porous n+ GaN. Furthermore, a high regrowth height was measured in the cross-section of approximately 200 nm. The desired regrowth was approximately 50 nm, so overall Regrowth 1 was not desirable.
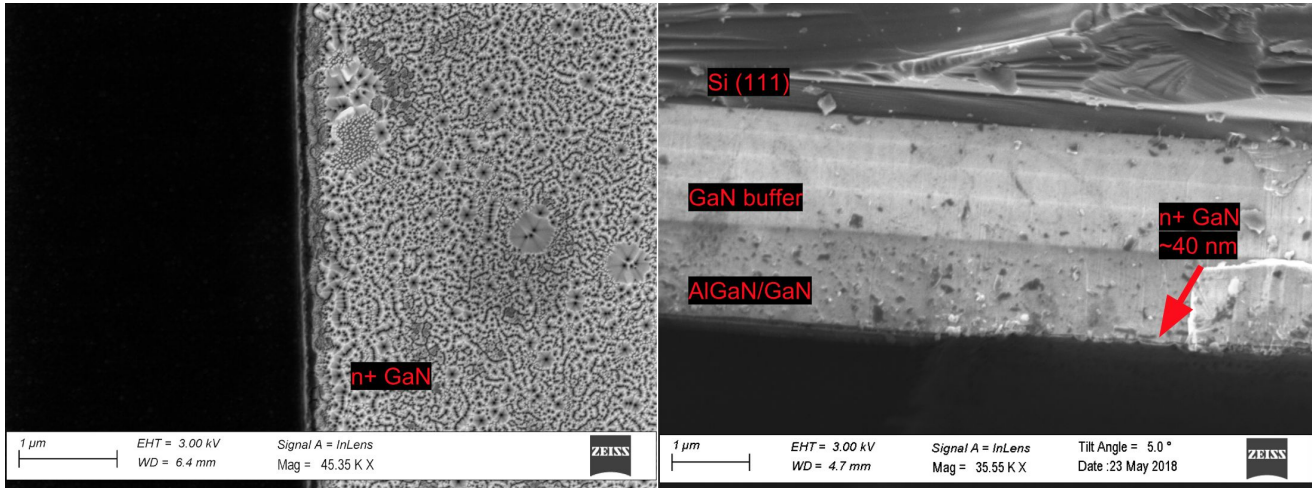

Figure 4: SEMs of the top view and cross-sections of Regrowth 2. The cross-section shows the various layers of the AlGaN/GaN stack. The measured growth was approximately 40 nm as shown in the SEM. The top view SEM shows the nonuniform, porous growth pattern of the regrown n+ GaN. The growth quality was thus determined to be poor.

Regrowth 2 exhibited the same non-uniform top level growth pattern. Numerous holes can be seen in the top view SEM of Figure 4. Though this poor growth was observed, a much lower growth height of approximately 40 nm was measured. This height was reasonably within our desired regrowth height of 50 nm.

Thus we chose to stick near the growth temperature for Regrowth 2 as we believed it would give us a height close to our desired nGaN growth height. Regrowth 3 was thus done at a slightly lower temperature of 1050 C and with the precursor flow rates doubled. Both the temperature change and precursor flow rate increase were chosen because it was believed that the porous nature of the regrowth was due to the high decomposition rates of the precursors at the high regrowth temperature of 1090 C. Thus by increasing the flow rates and slightly decreasing the temperature the growth should have been able to overcome the decomposition of the materials.

This hypothesis was shown to be correct in the SEMs of regrowth 3 (as seen in Figure 5).
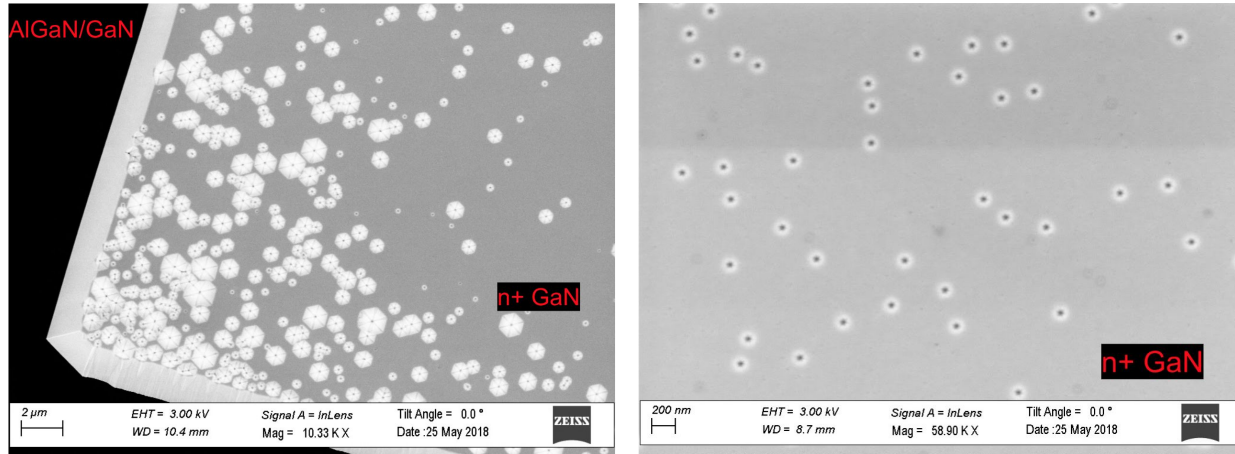
Figure 5: Top view SEMs of Regrowth 3. The left SEM is an image of a corner of one of the 150 um square trenches. Note the numerous hexagonally shaped holes. These holes can be attributed to defects within the crystal lattice of the n+ GaN regrowth. The right SEM is an image of a control sample in regrowth 3. The control sample was grown on a plain AlGaN/GaN stack. Looking at the control sample, it is clear that Regrowth 3 had much higher quality growth as the holes seen in Regrowths 1 and 2 are almost nonexistent.
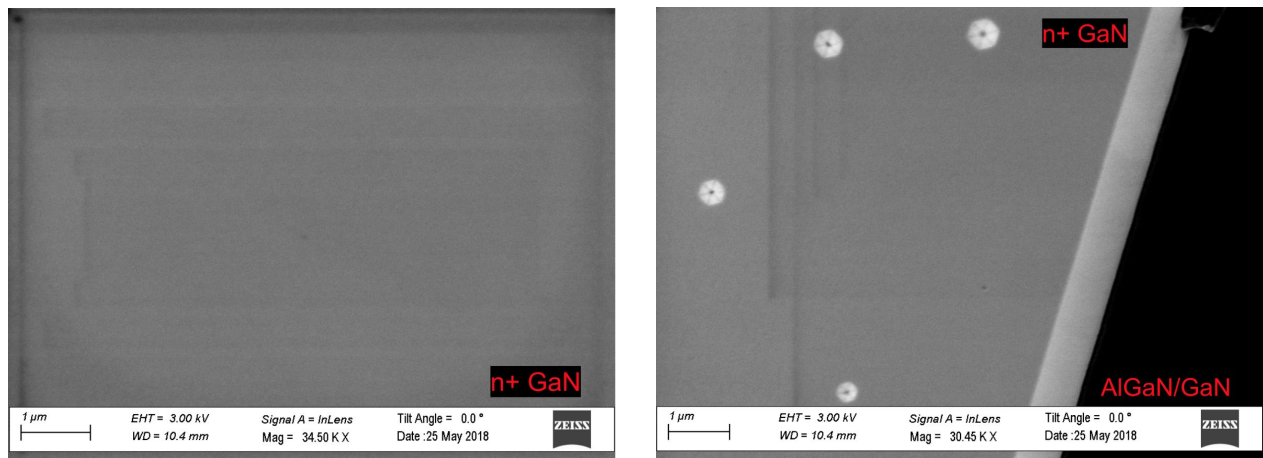
Figure 6: Top view SEMs of the edge versus center effect on the hexagonal defect holes. As can be seen the defects tend to occur near edges and corners while in the center of trenches in Regrowth 3 are nonexistent. This could be due to some etch roughness are some other nonuniformity leading to the defect.

As can be seen in Figures 5 and 6, the growth quality in Regrowth 3 is much higher. In Figure 5 we see that the overall growth is much more uniform than that of Regrowths 1 and 2. One can clearly see that the number and size of the holes within the the regrown nGaN has drastically decreased. The remaining holes exhibit hexagonal patterns indicative of defects

within the hexagonal crystal lattice of the nGaN. Furthermore these defects tend to appear near sidewalls and corners as opposed to centers of trenches as seen in Figure 6. The regrown nGaN for Regrowth 3 is therefore usable as ohmic contacts for HEMTs.

From here we ran another regrowth on a full die as detailed in Section IV. The below images are cross-sections of the observed growth in various angled trenches.
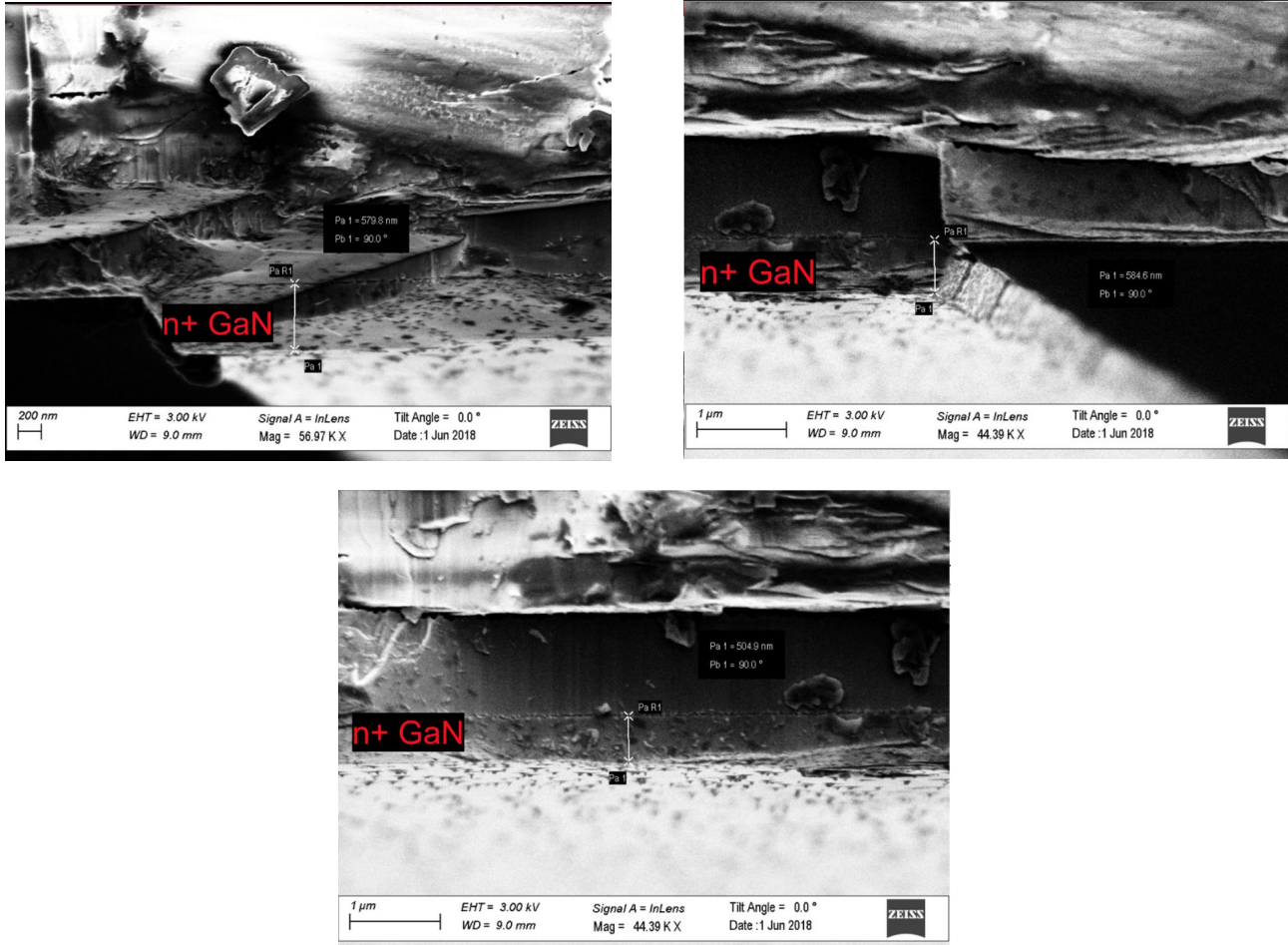

Figure 7: Cross-section SEMS of the vertical spiral trench in Regrowth 4. Notice the high growth height as well as the variation from center height to edge height. The vertical trench center was measured to be 504.9 nm while the edges were measured to be 584.6 nm on the right and 579.8 nm on the left.
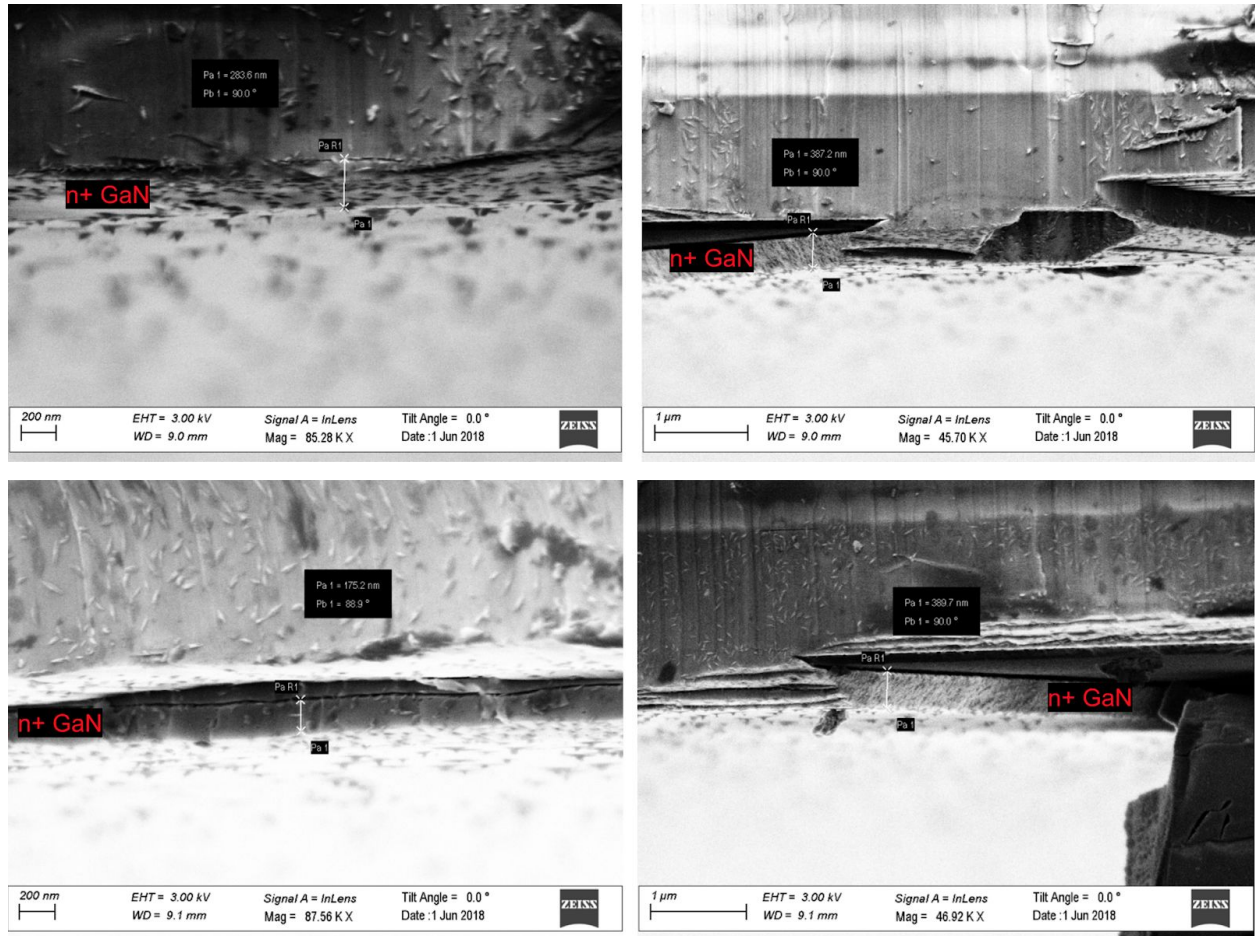
Figure 8: More cross-sectional SEMs of the spiral trenches 30 degrees from the vertical trench. We can clearly see here compared to Figure X the orientation dependence on growth as heights in the vertical trench were on the order of 500-600 nm while in these trenches are on the order 200-400 nm.

As seen in the above figures, the regrowth heights highly depend on the orientation of the trench. Furthermore, growth is increased by approximately 100 nm on the sidewall edges versus the center, something we expected to occur. Though we believed Regrowth 4 would have similar high quality growth as regrowth #3 because the same recipe was used, it seems that something went wrong either before the regrowth or after. The above images were taken post SiO2 etching and unexpected heights of ~600 nm were measured. We believe that these heights as well as the porous nature of the n+ GaN (as seen in the below Figure 9) could be attributed to carbon residue traces prior to MOCVD reentry or a thin film covering the surface that was unintentionally deposited during post-regrowth processing, such as during the SiO2 mask removal.
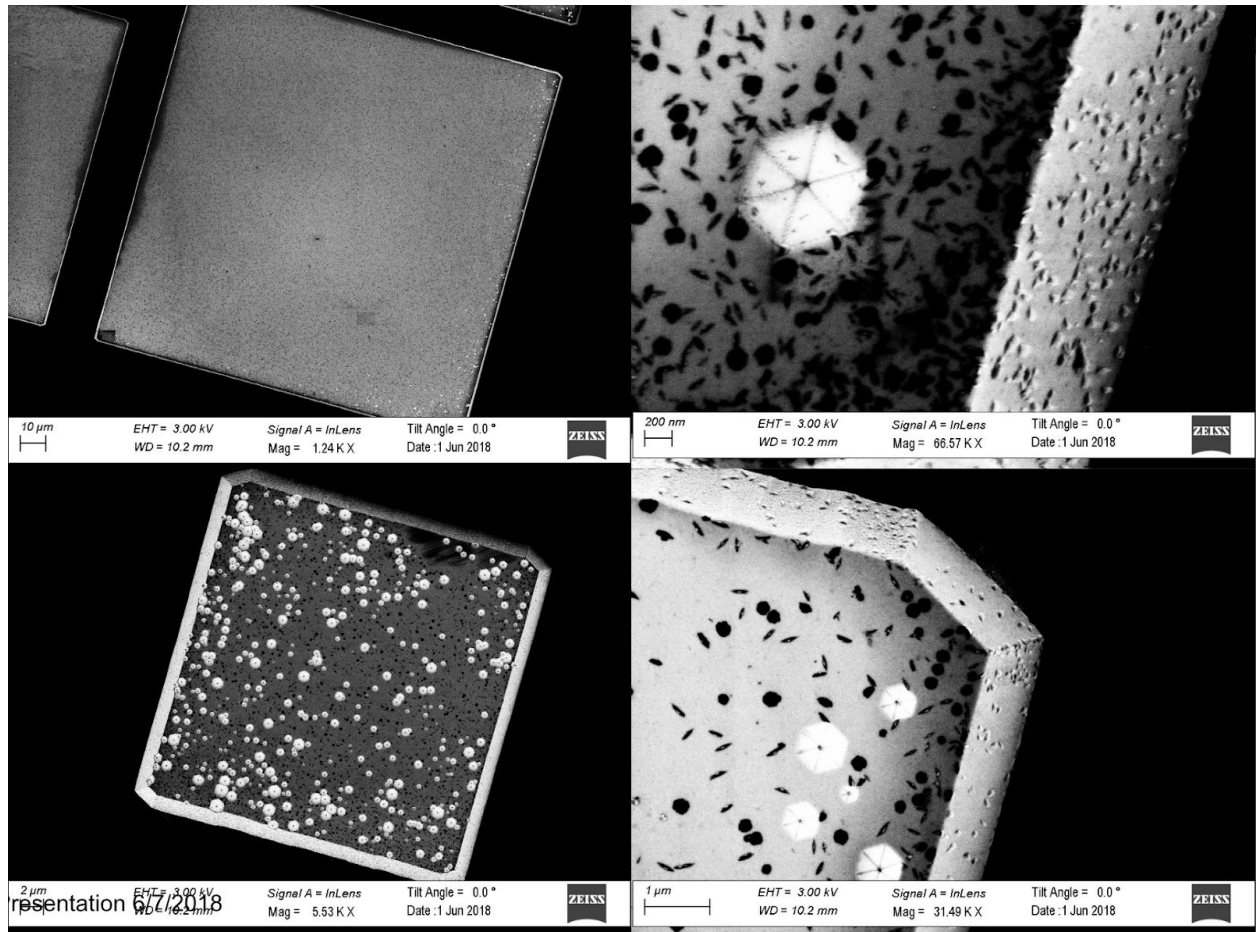
Figure 9: Top view SEMs of Regrowth 4. Notice the black marks and porous nature of the regrown nGaN. These marks and holes are thought to be attributed to carbon traces prior to reentry into the MOCVD.

VI. Electrical Data

Following microscopy, regrown samples #3 and #4 underwent additional processing in preparation for electrical characterization (steps 11-16). The Transfer Length Method or Transmission Line Method (TLM) technique was applied to regrown TLM structures in order to extract the contact resistance R_c, specific contact resistivity ρ_c, and the sheet resistance of our AlGaN/GaN heterostructure R_s. The measurements were performed as follows: one pair of contacts at a time was probed at a time. Voltage was applied and the resulting current was measured. The path of the current is through the first probe, into the metal contact, through the metal-semiconductor junction, across the semiconducting sheet, through the other metal-semiconductor junction and contact, and into the second probe. After data was collected

from each pair of contacts separated by a different distance, the total measured resistance versus the distance/length between contacts was plotted. From the plot, the sheet resistance and contact resistance can be directly determined - the sheet resistance is the slope of the curve fit divided by the width of the contact and the contact resistance is the y-intercept value divided by two (Fig. 10). Assuming the length of the contact is also known, the specific contact resistivity can be easily calculated the x-intercept, the linear transfer transfer length L. This technique assumes that the resistance of the contact metallization stack, i.e. the Ti/Al/Pt/Au, is negligible.
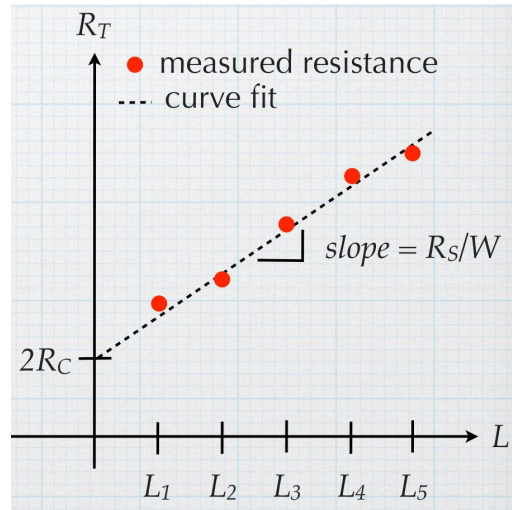
Figure 10: Demonstration of the TLM technique.
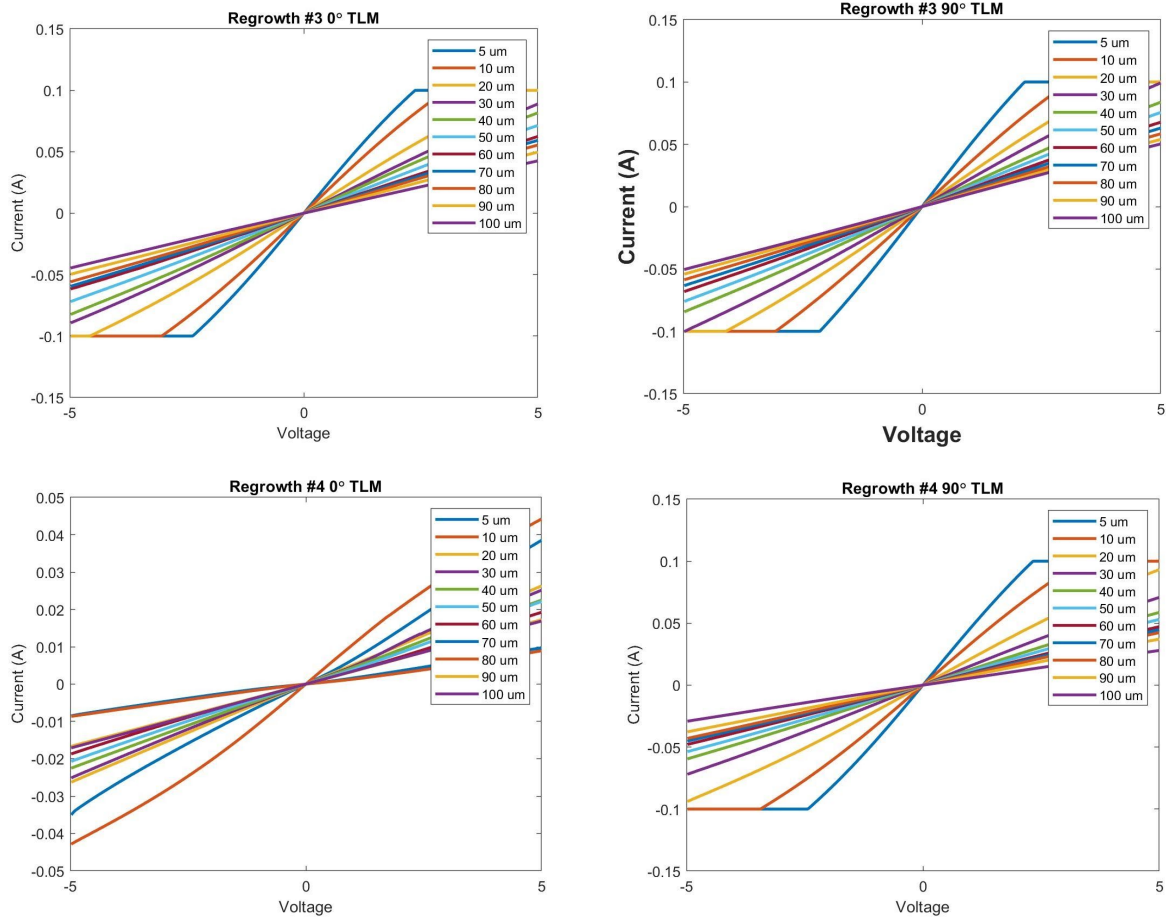
Figure 11: I-V measurements of TLM structures oriented 0 degrees and 90 degrees to the flat of regrown samples #3 and #4 for contact separation distances from 5um to 100um.
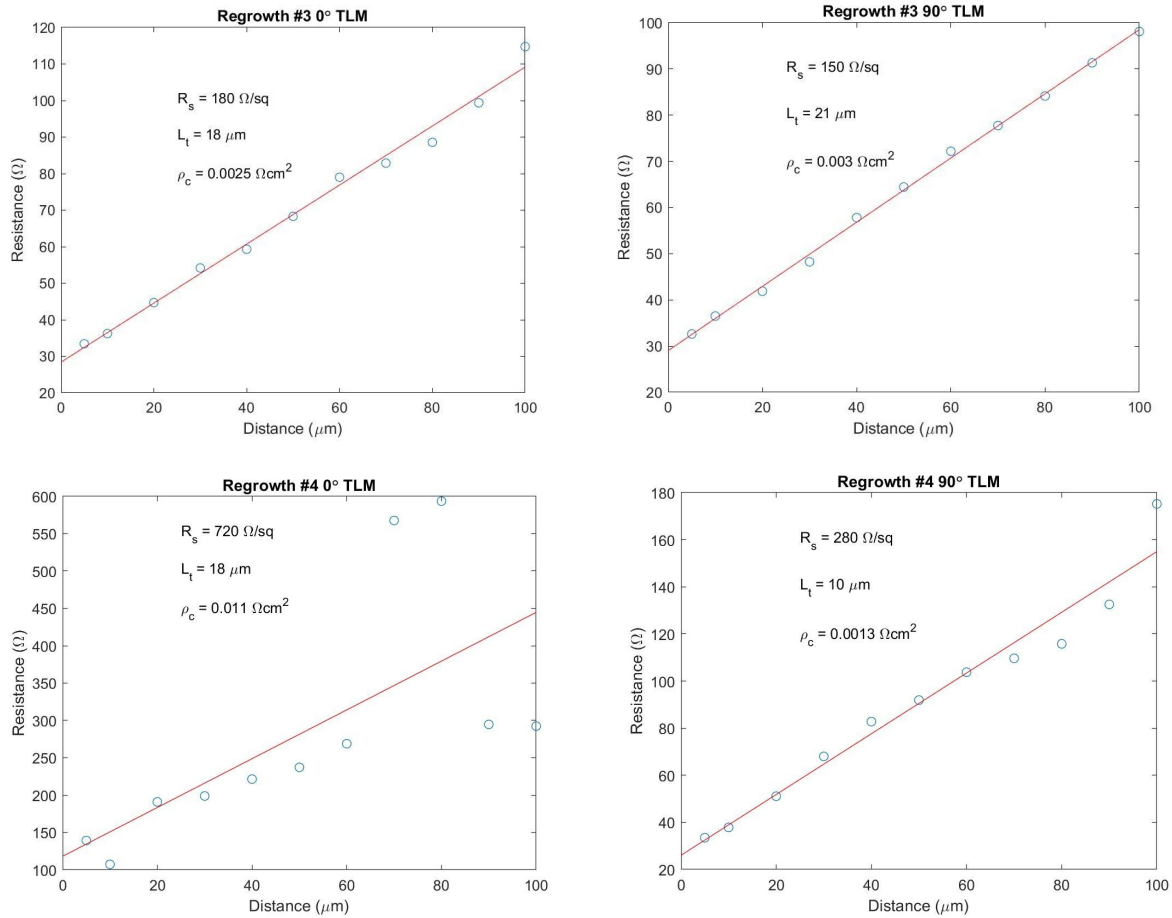
Figure 12: Resistance versus distance between contacts of TLM structures oriented 0 degrees and 90 degrees to the flat of regrown samples #3 and #4 for contact separation distances from 5um to 100um.

The I-V curves and Resistance vs. Distance plots are shown above for the TLM structures on regrowths #3 and #4 that were oriented 0 degrees and 90 degrees to the bottom of the sample when moving in a counterclockwise direction (Fig. 11, 12). The results are summarized in Table 2. It can be seen that the sheet resistance values for regrown sample #3 are similar and lower than average sheet resistance values for AlGaN/GaN heterostructures by ~200 Ω/sq, suggesting that the quality of the n+ GaN is high. The sheet resistance values for regrown sample #4 are inconsistent and this is likely due to the inconsistent and low quality of the n+GaN. The specific contact resistivities for all of the TLM structures measured were two to three orders of magnitude higher than the ~10^{-5} Ωcm^2 values achieved in standard, non-regrown Ohmic contacts to AlGaN/GaN, and four orders of magnitude higher than the state of the art regrown Ohmic contact resistivity values on the order of ~10^{-7} Ωcm^2 . [9,10] Yet considering the purity and doping concentration of the n+ GaN is much lower than anticipated for all of the samples in this study, the results are promising that future samples with higher doping concentrations and less carbon contamination could produce the desired contact resistivities.

Regrowth #	TLM Orientation	R_s (Ω/sq)	L_t (μm)	ρ_c (Ωcm^2)
3	0 degrees	180	18	2.5 x 10^{-3}
3	90 degrees	150	21	3.0 x 10^{-3}
4	0 degrees	720	18	1.1 x 10^{-2}
4	0 degrees	280	10	1.3 x 10^{-3}

Table 2: Summary of TLM measurement results.

Hall measurements were performed on both of the 1 cm x 1cm devices from regrowth #4, as seen on the right hand side of the sample design (Fig. 2). However, the results for the larger Hall structure that was entirely n+GaN (i.e no 2DEG present), were very inconsistent and therefore cannot be reported with confidence. The results from the Hall device with n+ GaN only under the contact pad regions and the AlGaN/GaN heterostructure intact elsewhere i.e. the 2DEG is present, are reported below in Fig. X. Two measurements were taken twice for verification. The mobility values are much lower than normally reported with the AlGaN/GaN MOCVD recipe used in this project, but Dr. Xiaoqing Xu has advised that similar values have been acquired in the SNF on samples where a 2DEG was present. With this information, it is concluded that the 2DEG does exist in regrown samples #4, but the acquired values are likely very low due to the poor quality of the n+ GaN and poor sidewall contact between the n+GaN and the AlGaN/GaN 2DEG. The sheet #, which is equivalent to the doping concentration, is five orders of magnitude lower than the 6 x 10^{18} cm^{-2} value that was desired, likely due to the carbon contamination of the samples interfering with the MOCVD n+GaN growth.

| Mobility (cm^2/Vs)	Sheet # (cm^{-2})	R_s (Ω/sq)	Carrier Type
4.39 x 10^2	6.55 x 10^{13}	2.22 x 10^2	Electrons

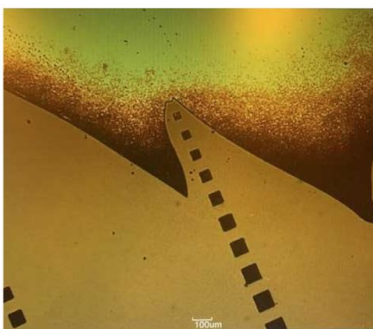|			
3.13 x 10^2	8.13 x 10^{13}	2.45 x 10^2	Electrons

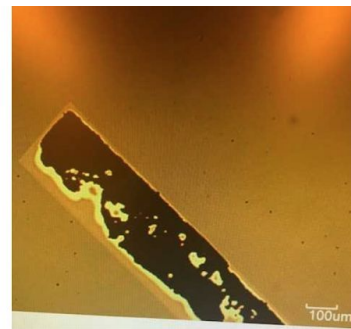**Table 3:** Summary of Hall measurements

VII. Conclusion

In conclusion we have presented our work in developing a regrowth process in the SNF MOCVD. Though after three regrowths we believed our process was successful, Regrowth 4 has given rise to doubts. It seems as though our samples could have run into one of two problems. Seeing the porous and high growth nature of Regrowth 4 SEMs we believe that either some carbon or other contaminant was not fully cleaned off prior to reentry into the MOCVD. As can be seen in Figure 13, optical microscope images of Regrowths 1 and 2 show that even in our early regrowths some unknown contaminant or residue was present.
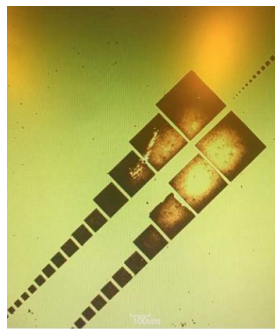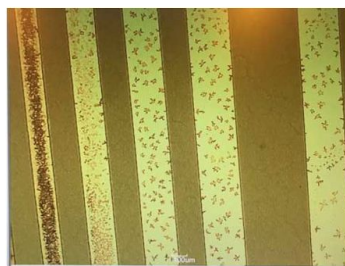

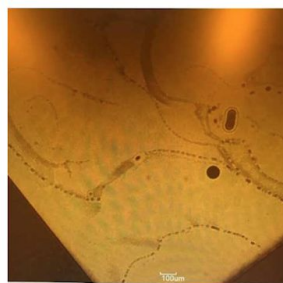Regrowth #2 Square patterns   Regrowth #1 Square patterns   Regrowth #1 Spiral Trench

Regrowth #2 Trenches   Regrowth #1 Large Hall

Figure 13: Optical microscope images of regrown regions of Regrowths 1 and 2. Notice the strange splotchy discoloration and polymer-like nature of certain regions. We believe that this is due to residual carbon polymers from prior processes that were not cleaned completely off prior to MOCVD reentry.

Future work will include a much heavier clean to ensure that this possible residue is removed prior to MOCVD regrowth.

VIII. Future Work

The regrown samples would benefit from secondary-ion mass spectrometry (SIMS) analysis to determine sample composition and verify the hypothesis of the presence of carbon traces during regrowth. Additionally, energy dispersive spectroscopy (EDS) on the regrown regions of sample #4 would provide information on the makeup of the n+GaN thin film. In order to further improve the Ohmic contact quality, the GaN etch recipe in the Oxford III-V should be optimized to produce smoother sidewalls in the recessed trenches where regrowth is to occur so proper nucleation of the GaN and better sidewall contact to the AlGaN/GaN can be achieved. Information on the orientation of the AlGaN/GaN with respect to the flat of the silicon (111) base wafer was lost during wet processing of the samples after dicing because no patterning or distinct marking was present on individual pieces. To recover the orientation information, X-ra diffraction (XRD) can be performed. The key improvement to this process in the future would be a more thorough clean of samples after processing following the original AlGaN/GaN growth but before re-entering the MOCVD chamber for regrowth to ensure polymers are not present during metal-organic chemical vapor deposition of n+ GaN. Furthermore, the log books for the Ox-RIE and Ox III-V will be examined to determine what materials were processed in the chambers prior to our own processing, in case we can find correlation between the substances used in their process and the contamination of our samples.

IX. Acknowledgements

X. References

[1] U. K. Mishra, P. Parikh and Yi-Feng Wu, "AlGaN/GaN HEMTs-an overview of device operation and applications," in *Proceedings of the IEEE*, vol. 90, no. 6, pp. 1022-1031, Jun 2002. doi: 10.1109/JPROC.2002.1021567

[2] D. Maier *et al*., "Testing the Temperature Limits of GaN-Based HEMT Devices," in *IEEE Transactions on Device and Materials Reliability*, vol. 10, no. 4, pp. 427-436, Dec. 2010. doi: 10.1109/TDMR.2010.2072507

[3a] Formation mechanism of Ohmic contacts on AlGaN∕GaN heterostructure: Electrical and microstructural characterizationsLiang Wang1, Fitih M. Mohammed1, *and* Ilesanmi Adesida1,2, a)

[3b] Ching-Hui Chen,a) Stacia Keller, Gia Parish, Ramakrishna Vetury, Peter Kozodoy, Evelyn L. Hu, Steven P. Denbaars, Umesh K. Mishra, "High-transconductance self-aligned AlGaN/GaN modulation-doped field-effect transistors with regrown ohmic contacts," Appl. Phys. Lett. 73, 1998.

[4] Sten Heikman, Stacia Keller, Steven P. DenBaars, Umesh K. Mishra, "Mass transport regrowth of GaN for ohmic contacts to AlGaN/GaN," Appl. Phys. Lett. 78, 2001.

[5] http://www.ee.ust.hk/~ptc/Papers/2012/Tongde_06467624.pdf

[6] Guo Hong-Yu et al 2015 Chinese Phys. Lett. 32 118501

[7] T. Huang, C. Liu, J. Bergsten, H. Jiang, K. M. Lau and N. Rorsman, "Fabrication and improved performance of AlGaN/GaN HEMTs with regrown ohmic contacts and passivation-first process," *2016 Compound Semiconductor Week (CSW) [Includes 28th International Conference on Indium Phosphide & Related Materials (IPRM) & 43rd International Symposium on Compound Semiconductors (ISCS)*, Toyama, 2016, pp. 1-2.

[8] Hou, M. and **Senesky, D.G.**, "Operation of ohmic Ti/Al/Pt/Au multilayer contacts to GaN at 600 °C in air," Applied Physics Letters, vol. 105, no. 8, 081905, 2014.

[9] Ganguly, S. , Song, B. , Hwang, W. S., Hu, Z. , Zhu, M. , Verma, J. , Xing, H. (. and Jena, D. (2014), AlGaN/GaN HEMTs on Si by MBE with regrown contacts and fT = 153 GHz. Phys. Status Solidi C, 11: 887-889. doi:10.1002/pssc.201300668

XI. Appendix A - SNF Community Service Report

MOCVD Regrown Ohmic Contacts to AlGaN/GaN Heterostructures

SNF Community Service Project Final Report

Savannah Benbrook Eisner (sbenbroo@stanford.edu)

Mentor: Dr. Xiaoqing Xu (steelxu@stanford.edu)

Motivation: Literature has demonstrated ohmic contact formation via MOCVD "regrowth" of an n+ GaN layer to side contact to the 2DEG on AlGaN/GaN substrates is a promising approach to reducing the contact resistance of GaN heterostructures [1][2][3]. Low Ohmic contact resistances on the order of tenths of Ohms/mm have been reported [4][5].

Objective & Background: The goal of this project is to refine the ohmic contact regrowth technique for GaN heterostructures that was previously began in E241 Spring 2018. During the E241 class, the fabrication process was developed to regrow ohmic contacts in the MOCVD (Appendix A), but SEM and optical microscopy images of the regrown samples have raised concerns of carbon residue from lingering hardened photoresist (See Appendix B). It was believed that the two consecutive dry etches the samples underwent in the Ox-RIE and the Ox-35 hardened the Shipley 3612 photoresist mask, rendering the wet processing removal after the etches and prior to MOCVD unsuccessful. The removal/clean consisted of a 90 second descum in the Drytek2 followed by 20 minute Piranha bath at 120C in clean beakers. Yet it did not appear that the pieces were entirely clean, as splotches could be seen by eye covering some of the trench areas. In hindsight, this was likely the hardened photoresist. In an attempt to remove the residual material, the samples were then soaked in SRS-100 for 20 minutes at 60C. The SRS-100 bath did not successfully remove the residue.

Results: The first objective of the SNF community service project was to remove what was believed to be hardened present on samples that went through the fabrication process flow up to MOCVD regrowth. These samples had not gone through the MOCVD regrowth yet due to the time restraints of the class. However, it was found that Drytek and Matrix photoresist removal recipes were unable to remove the residue from these samples, rendering them useless for MOCVD regrowth. These results indicate it is likely that the contamination was present PRIOR to regrowth, and so the n+GaN layer was grown over it and prevented removal. For instance,

extra Santolvac oil used to attach the sample pieces to a carrier wafer for Ox-RIE and Ox III-V etching could have adhered to the sample surface.

The fabrication process was restarted from the beginning with a fresh AlGaN/GaN-on-Si wafer grown in the MOCVD tool. However, after the regrowth step hairline cracks were seen in the AlGaN/GaN structure. We initially believed the cracks could be due to growing on a thinner Si <111> wafer (500 m) instead of the usual thicker Si <111> wafer (750 m), leading to higher stress levels in the wafer during the MOCVD growth and cooling process. However, subsequent growths also suffered from similar hairline cracks. Older samples of AlGaN/GaN wafers grown using the same recipe in the same reactor had no cracks except for the dies near the edge of the wafer, and usually only at one side (where the wafer edge is) of the piece. Thus, the conclusion was that something in the reactor changed in the last few months, either from contamination introduced into the chamber from a sample, Mg residue coming from the LED recipe, or just the accumulated reactor coating. Samples that had already gone through n+GaN regrowth were SEM images in areas where cracks were not present and showed a continuous thin film with only minor defects in the form of non-coalesced areas (Fig. 1 and 2). Thus, it was shown that the sample cleaning procedure prior to reentry into the MOCVD chamber is effective at removing contaminants. This indicates that the earlier "residue" seen on samples grown in the E241 class was due to a fabrication error and not an issue with the cleaning procedure.

Finally, metals were evaporated onto a sample that displayed hairline cracks and annealed to form Ohmic contacts to TLM structures in an attempt to see if the cracks actually impacted 2DEG quality (Fig. 3). Unfortunately, the sample yielded very high contact resistivities ~30 Ωcm^2, which is 9 orders of magnitude higher than the target value.
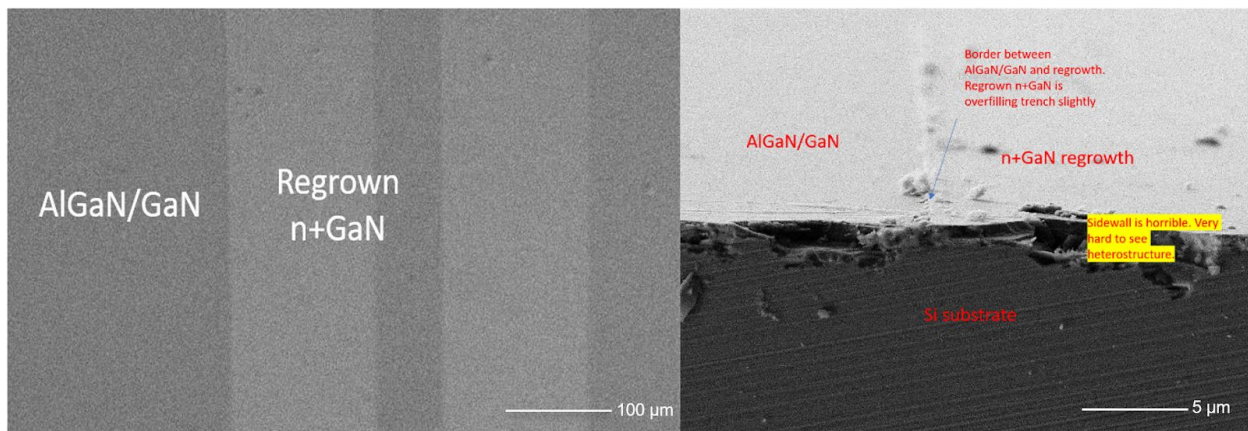
Fig 1. SEM images of n+GaN regrowth trenches in regions where hairline cracks were not present, showing continuous film (left) with some particles present on top due to cleaving. Cross-sectional image (right) shows overgrowth of regrown n+GaN film.
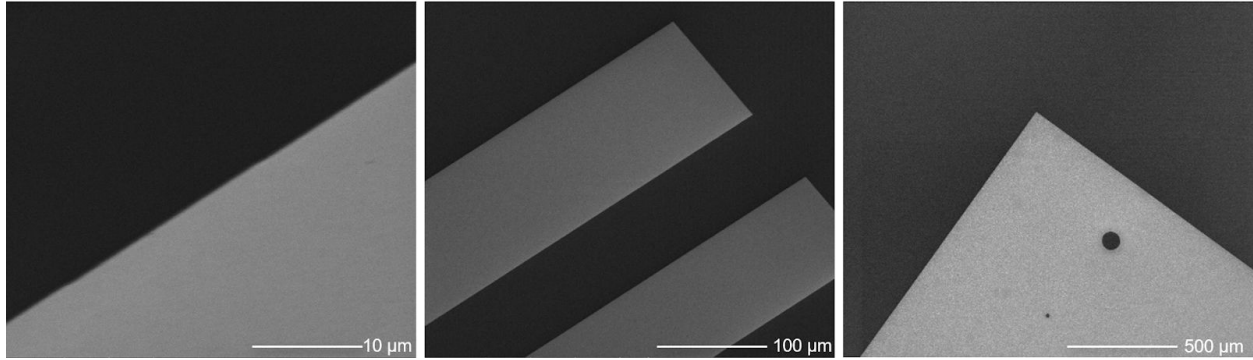
Fig 2. Additional SEM images of n+GaN regrowth trenches in regions where hairline cracks were not present, showing continuous film with only small areas where film did not coalescene properly (right).
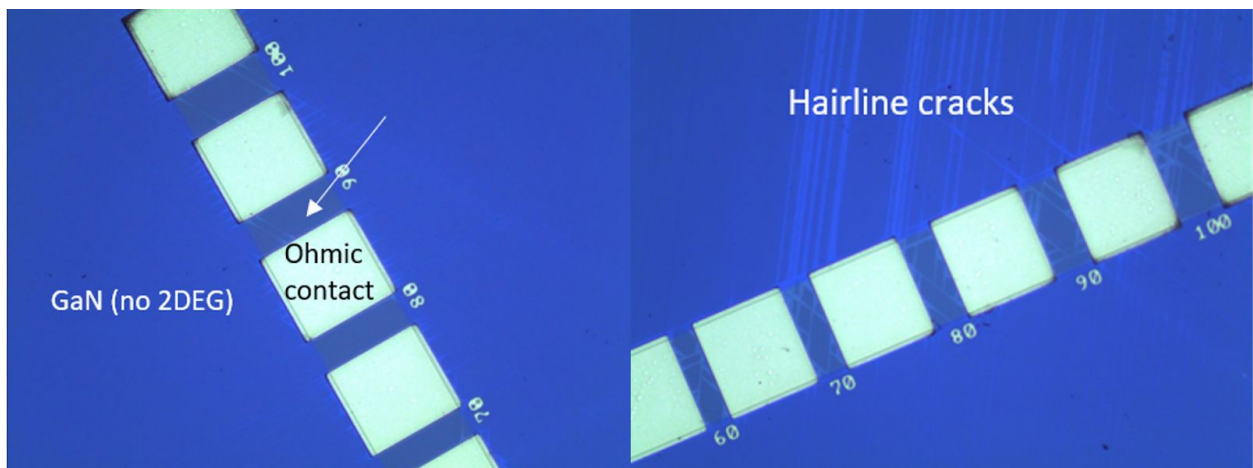
Fig 3. Optical microscope images of the fabricated TLM structures with n+GaN regrowth under Ohmic contact region. Hairline cracks are present in both the underlaying GaN layer and AlGaN layer

References

[1] Ching-Hui Chen,a) Stacia Keller, Gia Parish, Ramakrishna Vetury, Peter Kozodoy, Evelyn L. Hu, Steven P. Denbaars, Umesh K. Mishra, "High-transconductance self-aligned AlGaN/GaN modulation-doped field-effect transistors with regrown ohmic contacts," Appl. Phys. Lett. 73, 1998.

[2] Sten Heikman, Stacia Keller, Steven P. DenBaars, Umesh K. Mishra, "Mass transport regrowth of GaN for ohmic contacts to AlGaN/GaN," Appl. Phys. Lett. 78, 2001.

[3] http://www.ee.ust.hk/~ptc/Papers/2012/Tongde_06467624.pdf

[4] Guo Hong-Yu et al 2015 Chinese Phys. Lett. 32 118501

[5] T. Huang, C. Liu, J. Bergsten, H. Jiang, K. M. Lau and N. Rorsman, "Fabrication and improved performance of AlGaN/GaN HEMTs with regrown ohmic contacts and passivation-first process," *2016 Compound Semiconductor Week (CSW) [Includes 28th International Conference on Indium Phosphide & Related Materials (IPRM) & 43rd International Symposium on Compound Semiconductors (ISCS)*, Toyama, 2016, pp. 1-2.

XII. Appendix B - Project Runsheet

https://docs.google.com/spreadsheets/d/1X_bloNgfZ3qkJcghMvx07DT9vnR1r4CKM25CMzkafAY/edit?usp=sharing